JACS
JOURNAL OF THE AMERICAN CHEMICAL SOCIETY
Article
Cite This: J. Am. Chem. Soc. XXXX, XXX, XXX−XXX
pubs.acs.org/JACS

Molecular-Scale Structure of Electrode−Electrolyte Interfaces: The Case of Platinum in Aqueous Sulfuric Acid

Cheng Hao Wu,[†,‡,⊗] Tod A. Pascal,[§,⊗] Artem Baskin,[§] Huixin Wang,[‡,∥] Hai-Tao Fang,[‡,∥] Yi-Sheng Liu,[⊥] Yi-Hsien Lu,[‡] Jinghua Guo,[⊥,#] David Prendergast,[§] and Miquel B. Salmeron*[,‡,7]

[†]Department of Chemistry, University of California, Berkeley, California 94720, United States
[‡]Materials Science Division, Lawrence Berkeley National Laboratory, Berkeley, California 94720, United States
[§]The Molecular Foundry, Lawrence Berkeley National Laboratory, Berkeley, California 94720, United States
[∥]School of Materials Science and Engineering, Harbin Institute of Technology, Harbin 150080, P. R. China
[⊥]The Advanced Light Source, Lawrence Berkeley National Laboratory, Berkeley, California 94720, United States
[#]Department of Chemistry and Chemical Biology, University of California, Santa Cruz, Santa Cruz, California 95064, United States
[7]Department of Materials Science and Engineering, University of California, Berkeley, Berkeley, California 94720, United States

Supporting Information

ABSTRACT: Knowledge of the molecular composition and electronic structure of electrified solid−liquid interfaces is key to understanding elemental processes in heterogeneous reactions. Using X-ray absorption spectroscopy in the interface-sensitive electron yield mode (EY-XAS), first-principles electronic structure calculations, and multiscale simulations, we determined the chemical composition of the interfacial region of a polycrystalline platinum electrode in contact with aqueous sulfuric acid solution at potentials between the hydrogen and oxygen evolution reactions. We found that between 0.7 and 1.3 V vs Ag/AgCl the electrical double layer (EDL) region comprises adsorbed sulfate ions with hydrated hydronium ions in the next layer. No evidence was found for bisulfate or Pt−O/Pt−OH species, which have very distinctive spectral signatures. In addition to resolving the long-standing issue of the EDL structure, our work establishes interface- and element-sensitive EY-XAS as a powerful spectroscopic tool for studying condensed phase, buried solid−liquid interfaces relevant to various electrochemical processes and devices.

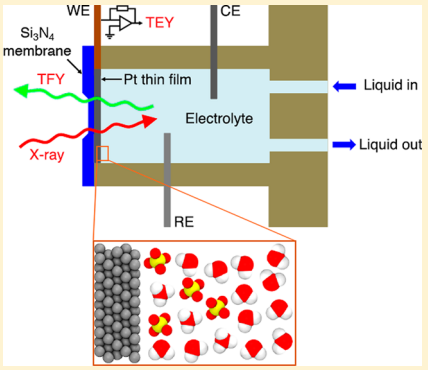

1. INTRODUCTION

Knowledge of the molecular structure and composition of solid−liquid interfaces is of fundamental importance for an atomic-level understanding of the interfacial processes of corrosion, geochemistry, atmospheric chemistry, (photo)electrocatalysis, and energy storage systems.[1−3] Renewed interest in interfaces and interfacial phenomena, due in part to the impetus for efficient storage of the energy produced by intermittent renewable sources, has spurred numerous studies using a variety of techniques, including electrochemical analysis,[2,4−6] radio-tracer methods,[7−9] electrochemical quartz crystal microbalance (EQCM),[10−12] and interface-sensitive microscopies and spectroscopies including scanning probe microscopy,[13] surface-sensitive vibrational spectroscopies,[14−16] surface X-ray scattering,[17,18] and surface-extended X-ray absorption fine structure (SEXAFS),[1] to name a few. However, interpretation of the data obtained with these techniques often relies on assumptions about the speciation and molecular structure of superficial layers based on thermodynamic arguments or models that have not been substantiated at the atomic level. As a result, understanding the dynamic molecular structure of buried functional electrochemical interfaces remains a great challenge.

Of particular interest is the prototypical interface between platinum and aqueous sulfuric acid [Pt−H_2SO_4(aq)]. Despite the substantial amount of data on Pt electrodes in numerous forms,[2,19,20] the interfacial composition and speciation at the Pt−H_2SO_4(aq) interface under various potentials remain unresolved. There is general consensus on the composition of the polycrystalline Pt−H_2SO_4(aq) interface at potentials E < 0.8 V vs RHE (or E_{RHE}).[7,15,16,21,22] In the anodic potential range (E_{RHE} > 0.8 V), however, the surface structure of the Pt electrode and the composition of the electric double layer (EDL) are still debated. In the conventional model, the evolution of the Pt−H_2SO_4(aq) interface is described as follows: (1) Initial adsorbates at the Pt−H_2SO_4(aq) interface at E_{RHE} > 0.8 V are assumed to be bisulfate (HSO_4^-) anions,[23] based on the fact that HSO_4^- dominates the speciation in dilute H_2SO_4 solutions, or a mixture of SO_4^{2-} and HSO_4^- coadsorbed with water and/or hydronium, a poorly defined system referred to as (bi)sulfate. (2) The (bi)sulfate species desorb with increasing anodic potentials, displaced by atomic oxygen (−O) and/or hydroxyl groups

Received: September 8, 2018
Published: October 29, 2018

DOI: 10.1021/jacs.8b09743
J. Am. Chem. Soc. XXXX, XXX, XXX−XXX

(−OH).[4−6,10,23−25] (3) Accumulation of −O/−OH at more positive potentials further excludes (bi)sulfate ions from Pt surface and leads to the formation of three-dimensional layers of $PtO_x/Pt(OH)_x$.[4−6,26]

Studies using previously mentioned characterization techniques have provided evidence supporting many aspects of the conventional model, but the picture of the Pt−H_2SO_4(aq) interface remains incomplete with several important questions unanswered, in particular, the chemical nature of the surface oxide/hydroxide. EQCM measurements[10−12] have confirmed mass addition onto the Pt surface at E_{RHE} > 0.8 V; however the assignment of the added mass typically relies on presumed speciation at the interface. X-ray scattering and SEXAFS experiments[18,27,28] successfully detected variations in electron density with increasing E_{RHE} to above 0.8 V, which were typically interpreted as resulting from surface oxide formation. Nevertheless, the electron density in this case is dominated by heavy elements, such as Pt, which makes these measurements less deterministic for light elements such as O or S.[35] S-Labeled radiotracer experiments[7−9] indicated that (bi)sulfate ions adsorb on the Pt surface around E_{RHE} ∼ 0.8 V and partially desorb at higher potentials, presumably replaced by surface oxide/hydroxide. Such a conclusion, especially on the sulfate adsorption, is also in line with a number of vibrational spectroscopy studies.[15,16,29,30] However, some in situ IR studies,[15,23,31,32] together with several single-crystal EC-STM measurements,[19,21] have called into question the formation of such a surface oxide. In addition, a recent surface-enhanced infrared absorption spectroscopy study[15] found that at anodic potentials the ν(OH) band of interfacial water molecules remains at ∼3000 cm^{-1}, instead of shifting to 3200 cm^{-1} as expected for water molecules forming hydrogen bonds with an oxide surface.

Recent technological advances have made it possible to extend powerful microscopy and spectroscopy characterization techniques, such as transmission electron microscopy, X-ray photoelectron spectroscopy (XPS), and X-ray absorption spectroscopy (XAS), from vacuum to ambient environments and under applied bias, thus providing new opportunities for *operando* investigation of solid−liquid interfaces.[3,33−36] Here, we use interface-sensitive electron-yield XAS (EY-XAS), based on measuring the drain current between solution and electrode resulting from the relaxation of core holes produced by absorption of X-rays.[3,33] The complexity of the absorption spectra, however, requires complementary first-principles electronic structure calculations for unambiguous interpretation. Here, we apply this approach and extend it by including multiscale simulations to elucidate the long-standing question of the interfacial composition and speciation at the Pt−H_2SO_4(aq) interface. Our measurements and calculations indicate that under anodic potentials preceding oxygen evolution the interface region (1−2 nm) is dominated by adsorbed sulfate ions (SO_4^{2-}), hydronium ions, and solvating water. In contrast to the conventional "oxide formation" model, we found no trace of Pt−O/Pt−OH or bisulfate (HSO_4^-) species within the sensitivity limit of the measurements. Our results call for a review of models of electrochemical interfaces based on conventional experimental methods that do not involve unambiguous, interface-sensitive spectroscopy.

2. EXPERIMENTAL SECTION

Thin films (∼15 nm) of Pt (or Au) working electrodes were deposited via e-beam evaporation onto X-ray transparent Si_3N_4 membrane windows (100 nm in thickness). Prior to film deposition, a 2 nm Ti layer was deposited, also by e-beam evaporation, to act as an adhesion layer between the Si_3N_4 surface and the metal film. The films were polycrystalline with 2 nm average corrugation, as shown by the AFM topographic images (Figure S1). The metal-covered Si_3N_4 window was then assembled in a liquid cell,[33] containing a Pt wire acting as a counter electrode and a miniature Ag/AgCl reference electrode (∼0.25 V vs RHE in 0.05 M H_2SO_4). *Operando* XAS measurements were performed at BL8.0.1.3 of the Advanced Light Source synchrotron facility at the Lawrence Berkeley National Laboratory. Bulk-sensitive total fluorescence yield (TFY) and interface-sensitive total electron yield (TEY) XAS spectra were collected simultaneously during each experiment.

Concurrent first-principles molecular dynamics (FPMD) calculations were performed, with the Pt electrode modeled by a 4 × 4 × 6 supercell of 96 atoms, with the (111) surface exposed to an aqueous solution comprising 119 water molecules and various amounts of sulfuric acid species (H_2SO_4, HSO_4^- and SO_4^{2-}), neutralized by appropriate amounts of H_3O^+ molecules. Umbrella sampling[37,38] free energy calculations were performed to determine the binding free energy of the individual sulfuric acid species to the Pt electrode. A description of the EDL at various surface charge densities with open-boundary conditions was obtained from a self-consistent continuum model, based on a free energy functional and a modified Poisson−Boltzmann equation formalism.[39] Input parameters for the continuum model were provided by FPMD calculations. The simulated K-edge XAS of the various oxygen containing species were obtained using the eXcited electron and Core−Hole method,[40] critically employing a self-consistent energy alignment scheme[41] that allows us to unambiguously resolve the absolute XAS peak positions of different oxygen containing species in the unit cell.

More details regarding the experimental setup and computational procedure are described in the Supporting Information.

3. RESULTS AND DISCUSSION

3.1. XAS at the Pt−H_2SO_4(aq) Interface. Using the liquid cell shown schematically in Figure S1 for *operando* EY-XAS measurements, we collected cyclic voltammograms (CV) of our Pt electrode in 0.05 M H_2SO_4 (Figure S2). The CV is very similar to those published for polycrystalline platinum electrodes.[2] Notably, between hydrogen desorption and oxygen evolution potentials a broad anodic wave starting around E = 0.6 V vs Ag/AgCl (corresponding to E_{RHE} ∼ 0.85 V) is observed, followed by a strong peak around $E_{Ag/AgCl}$ = 0.5 V in the cathodic sweep. These features have been commonly attributed to Pt oxide formation or −O/−OH adsorption and oxide reduction, respectively.[2,4,10,42]

Under open-circuit potential (OCP; typically 0.3−0.4 V vs Ag/AgCl for a fresh Pt film), the O K-edge EY-XAS spectrum is similar to that found at the interface of the Au−H_2O system,[33] showing a substantial suppression of the pre-edge feature at 535 eV (due to preferential water orientation and orbital hybridization with the metal substrate) compared to the bulk XAS spectra of pure water and H_2SO_4 solution (TFY spectra in Figure S3). Such similarity indicates that at OCP the Pt−H_2SO_4(aq) interface is dominated by water. This conclusion is supported by our equilibrium first-principles molecular dynamics (FPMD) simulations which reveal that the water density profile across the Pt−H_2SO_4(aq) interface in a 0.4 M H_2SO_4 solution is similar to that of Pt−H_2O and Au−H_2O interfaces, with the first layer mass density peak at ∼3 Å (Figure S4). At the Au−H_2O interface we also observed that negative bias potentials modify the hydrogen-bonding network by increasing the fraction of water molecules with broken hydrogen bonds, resulting in a pronounced pre-edge feature.[35] We find a similar effect at both Pt−H_2SO_4(aq) and Au−H_2SO_4(aq) interfaces at voltages below the OCP (Figures S5 and S6).

In the potential region more positive than the OCP ($E_{Ag/AgCl}$ > 0.3 V), the O K-edge EY-XAS spectra of the Pt−H_2SO_4(aq) interface species (Figure 1a) exhibit a pre-edge peak at 535 eV.

DOI: 10.1021/jacs.8b09743
J. Am. Chem. Soc. XXXX, XXX, XXX−XXX

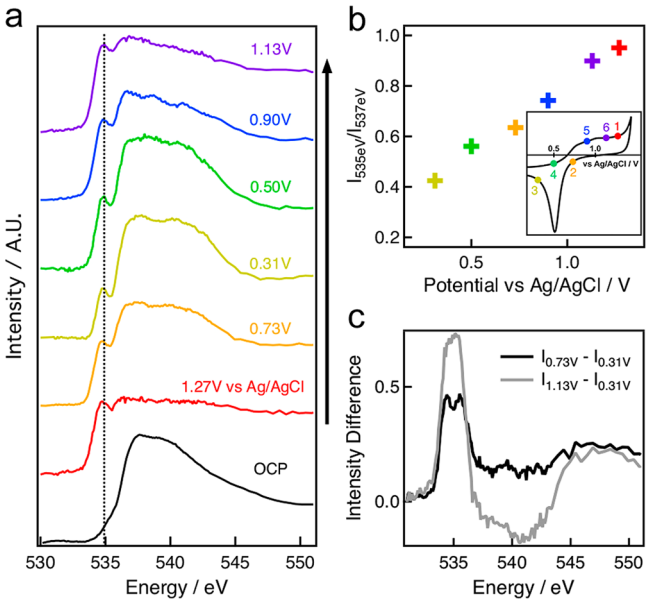

Figure 1. *Operando* XAS measurements at the Pt−H_2SO_4(aq) interface at open circuit and anodic potentials. (a) O K-edge EY-XAS spectra at different potentials. (b) Variation of the intensity ratio between the prepeak (535 eV) and the main peak (537 eV) as a function of potential. The color of each data point matches the color of the spectrum from which the value was calculated. The inset shows the anodic part of the Pt−H_2SO_4(aq) CV curve (full-range CV shown in Figure S2). The colored number indicates the order of the spectra acquisition. (c) Differences between the spectra measured at 0.73 and 0.31 V and 1.13 and 0.31 V (vs Ag/AgCl), respectively.

The position of this peak coincides with the pre-edge peak of water with broken hydrogen bonds, visible both in the spectra of bulk water and under negative potentials at the Au−H_2O interface, but notably absent under positive potentials. However, the pre-edge peak at the Pt−H_2SO_4(aq) interface is narrower than the pre-edge feature at the Au−H_2O interface (Figures S6 and S7), which appears as a shoulder in XAS spectra obtained using the same apparatus with identical settings. Moreover, Figure 1a shows that the pre-edge peak observed at the Pt−H_2SO_4(aq) interface at positive potentials becomes more intense with respect to the main edge peak (537 eV) at higher potentials. These changes are reversible, as shown by the potential-dependence of pre-edge-to-main-edge ratio (I_{535eV}/I_{537eV}) (Figure 1b and Figure S8): From 1.27 to 0.31 V and back to 1.13 V, the ratios follow roughly the same trend. Another variation in the spectra is the extension of the XAS postedge plateau (>540 eV) toward higher energy at more positive potentials, as exemplified by the intensity difference between spectra collected at 0.73 and 1.13 V, and that at 0.31 V (Figure 1c), where a broad feature can be discerned above 540 eV. At the highest potentials examined, 1.13 and 1.27 V, the spectra exhibit a more extended flat tail that resembles saturation effects commonly observed in fluorescence or low-energy partial electron yield XAS.[43] This could be the result of a substantial amount of low energy secondary electrons generated deeper in the solution reaching the electrode at higher positive potentials. As discussed in the Supporting Information (SM), however, this effect is not severe enough here to distort the EY-XAS spectra, at least for positive bias below ∼1 V.

3.2. Speciation and Ion Distribution at the Pt−H_2SO_4(aq) Interface. To provide a molecular-scale model of the Pt−H_2SO_4(aq) interface, we performed FPMD simulations paired with continuum thermodynamic models. From this we determined which of the multiple species, H_2O, H_3O^+, SO_4^{2-}, HSO_4^-, and H_2SO_4,[44] are most likely to be present at the interface and contribute to the overall O K-edge spectra and, thus, facilitate the interpretation of XAS spectra. The simulations revealed that in contact with low concentration of H_2SO_4 (∼0.4 M in the simulation, Figure 2a), the dominant species on the neutral Pt surface are water molecules. A small number of sulfate anions reside close to the surface (∼2.7 Å) together with a small amount of H_3O^+ in the neighboring water layer (8−10 Å). These results are in qualitative agreement with 0K DFT calculations of sulfuric acid anions on Pt(111).[45] We note that even at this relatively low concentration in the simulation cell the sulfate anions preferentially adsorb near the interface. For more concentrated H_2SO_4 solutions (∼3.0 M in the simulation), we find that sulfate ions displace interfacial water molecules, such that the surface density of sulfate anions surpasses that of water, with a concomitant increase in H_3O^+ concentration in the first interfacial layer (1.5−4.3 Å), as shown in Figure 2b. This is in line with free energy calculations in the thermodynamic (infinite time) limit shown in Figure S9a, which show a minimum at ∼2.7 Å from the Pt surface in the free energy profile of solvated SO_4^{2-} ions (similarly for HSO_4^- and H_2SO_4). Notably, the calculated binding free energy of an isolated SO_4^{2-} ion to the interface is a relatively weak −34.8 kJ/mol/molecule at 298 K. This is comparable to experimental estimates based on isotherms at equilibrium (∼80%) surface coverage[26] of ∼350 kJ/mol or, equivalently, 35−45 kJ/mol. Further, for the charge-neutral surface, our FPMD simulations further show that the adsorbed sulfate ions act as free rotors near the Pt interface, consistent with the experimental observation that at the potential of zero charge (PZC) (0.16 V vs RHE) the S−O stretching frequencies of the adsorbed sulfate ions coincide with those of free ions.[23] At higher positive surface charge (i.e., more anodic potential), we expect increased population and more specific binding of the sulfate anions, as observed experimentally.[21,46]

We note that FPMD simulations have certain limitations in predicting molecular speciation at interfaces and realistically modeling biased interfaces, which arise from the periodic boundary and neutrality conditions used in the simulations, as well as the finite number of species in the simulation cells, and limited computation time. We overcome these limitations by developing a self-consistent continuum model (details in the Supporting Information and Figures S10 and S11), which provide information about the distributions of ions for open systems under applied bias (Figure 2c and Figure S12). As shown in Figure 2c and consistent with our FPMD simulations, this model predicts that although in the calculation the bulk concentration of H_2SO_4 was set to 0.05 M, the interface concentration of sulfate and bisulfate species is substantially higher, even on the charge-neutral surface. With increasing charge density on the electrode (or equivalently external bias), the surface density of HSO_4^- increases initially followed by a slow decay, as more SO_4^{2-} ions are attracted to the interface, eventually becoming the dominating surface species (Figure 2c and Figures S12 and S13). These anions expel water molecules in the EDL and create a local environment with a higher pH than in the bulk solution.

Finally, we note that our FPMD calculations also indicate that the adsorption and accumulation of sulfate ions at the interface alters the hydrogen-bonding network of interfacial water molecules. We performed hydrogen bond statistical analysis, with the hydrogen bond defined by the method prescribed by Luzar and Chandler.[47] For each water molecule, we separately considered

DOI: 10.1021/jacs.8b09743
J. Am. Chem. Soc. XXXX, XXX, XXX−XXX

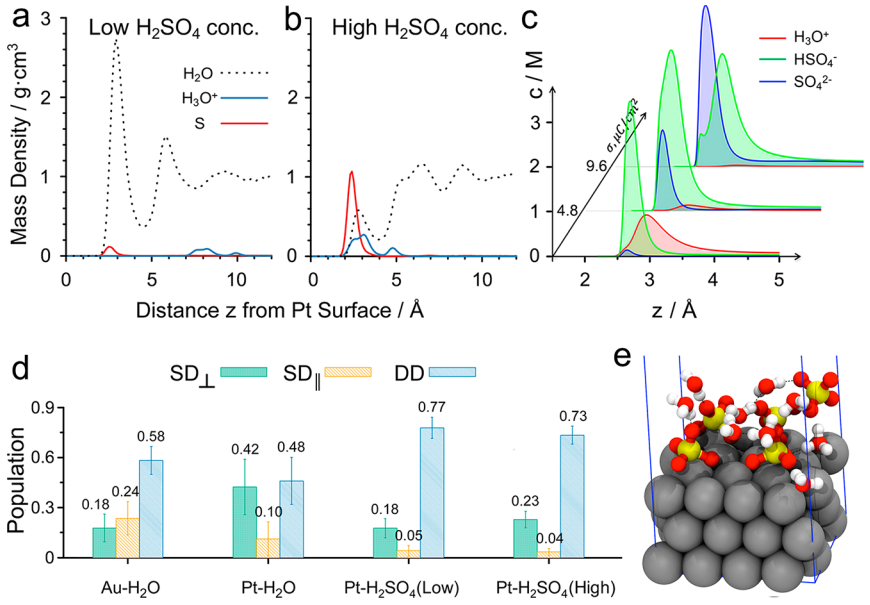

Figure 2. Structure of the Pt−H_2SO_4(aq) interface from first-principles molecular dynamics (FPMD) and thermodynamic multiscale simulations. (a, b) Surface mass density profile of H_2O, H_3O^+, and S in (a) low concentration (0.4 M in the simulation cell) and (b) high concentration (3.0 M in the simulation cell) sulfuric acid solutions. (c) Ion concentration profiles near a Pt electrode at various surface charge densities from the continuum model with bulk H_2SO_4 concentration of 0.05 M. (d) Populations of water species of single and double donors with configurations perpendicular and parallel to the surface ($SD_\perp$, $SD_\parallel$, DD) at interfaces between Au−H_2O, Pt−H_2O, and Pt−H_2SO_4 in 0.4 and 3.0 M H_2SO_4 solution. (e) Representative snapshot of sulfuric acid at the Pt interface at high surface coverage (~84%). Water molecules beyond 0.5 nm of the interface are removed for clarity.

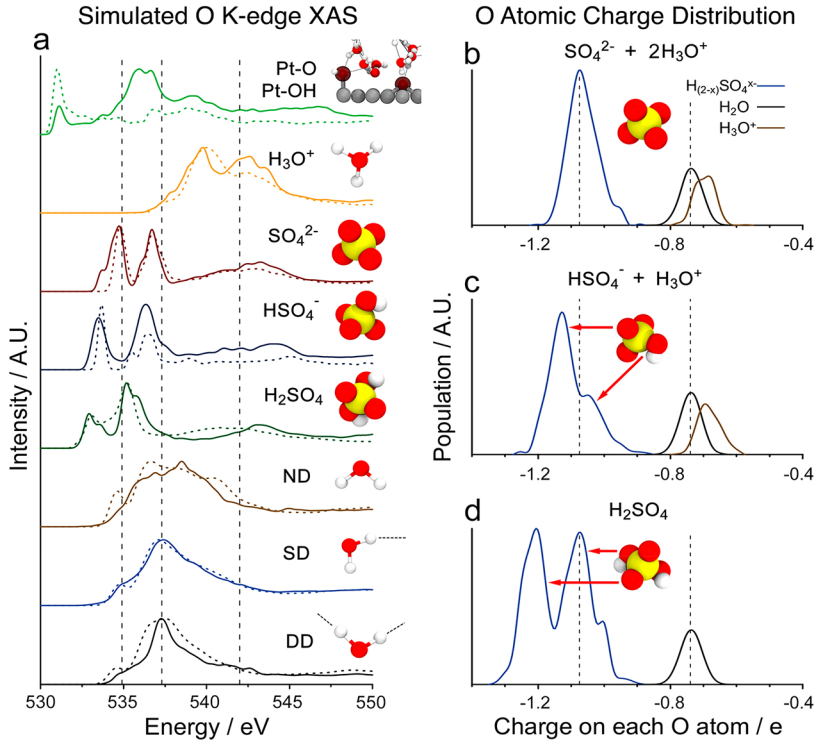

Figure 3. Electronic structure and XAS simulations. (a) O K-edge XAS spectra of various O-containing species at the Pt−H_2SO_4(aq) interface calculated from first principles. The XAS of each species at the interface (solid line) is compared to that in the bulk (dashed lines). Dashed vertical lines represent the energy of the three main XAS features of bulk water: the pre-edge near 535 eV, the main edge near 537 eV, and the postedge near 541 eV. (b−d) Charge distribution on the oxygen atoms in the various solvated sulfate species (blue), bulk water (black), and H_3O^+ (brown) from Bader charge analysis of bulk systems. Dashed vertical lines indicate the average partial charges on each oxygen atom in the SO_4^{2-} ions (−1.07e$^-$) and in water molecules (−0.74e$^-$).

those with both hydrogens participating in hydrogen bonding with neighboring water molecules (double donors, or DD), those with one broken hydrogen bond (single donors) that are aligned either perpendicular (SD⊥) or parallel (SD||) to the Pt surface, as well as those with two broken hydrogen bonds (nondonor, or ND). As shown in Figure 2d, sulfate adsorption at

DOI: 10.1021/jacs.8b09743
J. Am. Chem. Soc. XXXX, XXX, XXX−XXX

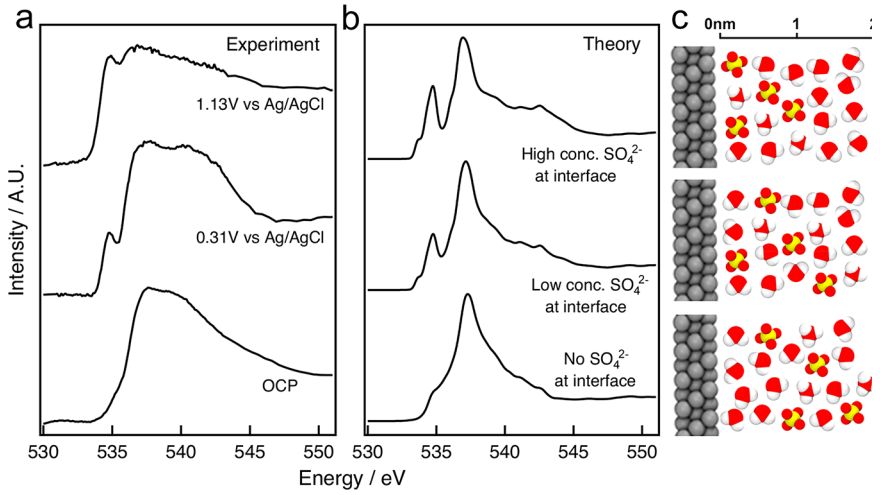

Figure 4. Comparison between experiment and theory. (a) Experimental O K-edge XAS spectra of the Pt−H_2SO_4(aq) interface measured at OCP, 0.31 and 1.13 V vs Ag/AgCl. (b) Composite simulated XAS spectra of Pt−H_2SO_4(aq) interface where there is no sulfate, low concentration, and high concentration of sulfate, respectively, based on the speciation from equilibrium FPMD simulations. (c) Molecular illustrations of the electrical double layer region of the Pt−H_2SO_4(aq) interface for three interfacial sulfate concentrations: low, medium, and high.

the Pt surface promotes hydrogen bonding, leaving more fully coordinated water molecules (DD species; 73−77% depending on concentration) compared to the case without sulfate ions (48%), as shown in Figure 2d.

3.3. First-Principles Simulated XAS of the Pt−H_2SO_4(aq) Interface. Having determined the thermodynamic average speciation and molecular configurations at the interface we can deduce what molecular structural motifs give rise to the spectral signatures observed in experiment. To our knowledge, no experimental O K-edge spectra have been obtained for solvated sulfate or hydronium species in the bulk solution, due to overwhelming signal from bulk water molecules. XAS spectra of sulfate salt crystals (Figure S14) are not meaningful in this context because the electronic structure of the sulfate ions confined in a crystal matrix is different from that of mobile sulfate ions hydrogen bonded to surrounding water molecules. Similarly, the XAS of highly concentrated H_2SO_4 is of little use due to the drastically different dissociation mechanism and coordination chemistry when very few water molecules are present. Moreover, electronic interactions between adsorbate and substrate can modify the XAS, as illustrated in the case of the Au−H_2O interface.[33] Therefore, first-principles XAS calculations[40] based on a self-consistent energy alignment scheme[41] were performed to provide atomic-scale insights into the molecular structure and electronic transitions that give rise to the observed spectra.

Figure 3a presents the simulated XAS of the various species, including solvated H_3O^+, H_2SO_4, HSO_4^-, and SO_4^{2-}, as well as H_2O molecules with different configurations (DD, SD, or ND), both in the bulk solution and at the Pt−H_2SO_4(aq) interface. We find that H_2O molecules at the Pt interface have XAS signatures similar to those at the Au interface, where the intensity of the pre-edge feature at 535 eV related to SD species is suppressed due to delocalization of the molecular orbitals of excited H_2O molecules into the metal substrate.[33] On the other hand, the XAS features of solvated H_3O^+ ions, which are located in the second solvation layer and are thus not electronically coupled to the metal band structure are blue-shifted to the region above 537 eV compared to those of water, reflecting the core-level chemical shift due to the additional H^+ (Figure 3b,c).

The simulated XAS of the SO_4^{2-} anion is characterized by two prominent peaks at 534.5 and 537 eV, which align closely to the pre-edge and main-edge peaks of bulk water. These XAS spectral signatures do not shift appreciably with different amounts of positive surface charge on the Pt-electrode (Figure S15). A similar pair of prominent peaks are present in the simulated spectrum of the solvated HSO_4^- ion but red-shifted to ∼533 and ∼536 eV and would be clearly distinguishable from the SO_4^{2-} spectrum. Analysis of the ground-state electron density (Figure 3c) of the solvated HSO_4^- ions reveals an asymmetric charge distribution among the four oxygen atoms: the three nonprotonated oxygen atoms have increased electron charge density (−0.05e on average), whereas the oxygens in the −OH group have slightly less electron density (+0.01e on average) compared to SO_4^{2-}. This splits the degeneracy and results in an additional pair of blue-shifted features at ∼534 and ∼537 eV associated with excitations involving oxygen atoms in the −OH group. However, the −OH group actively participates in hydrogen bonding with the surrounding water molecules, and the resulting core-excited state is delocalized over several molecules. Such delocalization substantially reduces its XAS intensity and makes the feature at 534 eV completely overwhelmed by a main peak of nonprotonated oxygen atoms at 533 eV. The simulated XAS of H_2SO_4 species next to the Pt interface show quantum mechanical effects even more pronounced than in HSO_4^-, manifested in the red-shift to 532.5 and 535.5 eV of the peaks associated with nonprotonated oxygen atoms. Similarly, because of the increased electron density on these atoms in the ground state, the excitations involving the protonated oxygen atoms display two prominent shoulders at energies slightly higher than the main peaks.

The simulated XAS of solvated Pt−O/Pt−OH species, at the top of Figure 3a, exhibit a distinctive spectroscopic signature: a sharp peak at ∼531 eV, resulting from O1s → hybridized O2p-Pt5d transitions. These spectral features are prominent because the core-excited states are localized along the Pt−O(H) bonds, which are primarily ionic with occupied orbitals that lie deep in the valence band. These calculated Pt−O(H) XAS spectra are consistent with experimental partial electron yield XAS results from various surface Pt oxides measured with ambient-pressure XPS under partial pressure of O_2 gas.[48]

3.4. Structure of the Pt−H_2SO_4(aq) Interface at Anodic Potentials. Our multiscale theoretical analysis of the thermodynamics and corresponding XAS simulations provides

DOI: 10.1021/jacs.8b09743
J. Am. Chem. Soc. XXXX, XXX, XXX−XXX

strong evidence for the preferential adsorption of sulfate species at the Pt−H_2SO_4(aq) interface, especially at positive potentials. The increase in the surface density of both SO_4^{2-} and H_3O^+ ions obtained in the simulations is in line with the observed growth of the sharp peak around 535 eV and the features at and above 540 eV, as illustrated in the composite simulated XAS spectra using the speciation from our equilibrium FPMD simulations at various sulfate concentrations (0, low, and high; Figure 4b) with the experimental XAS spectra at different potentials (OCP, 0.31 V, and 1.13 V vs Ag/AgCl; Figure 4a). The pre-edge feature observed at anodic potentials originates from the SO_4^{2-} ions alone, with no contribution from interfacial H_2O molecules. This is because the H_2O reorientation behavior at the positively charged surface results in a suppressed prepeak, as demonstrated in the case of Au−H_2O.[33]

Of particular interest is the lack of evidence for the existence of Pt−O(H) layers in our experimental spectra, even at the highest potential tested here ($E_{Ag/AgCl}$ = 1.27 V). This finding goes against the widely accepted model of competitive replacement of adsorbed anions by oxygenated species and formation of oxide/hydroxide at the Pt−H_2SO_4(aq) interface at E_{RHE} > 0.8 V. It is also hard to justify the desorption of sulfate anions from the more positively charged surface due to competitive −O(H) adsorption.[8,26] Given the relatively weak Pt−OH_{ads} bonding compared to the strength of the Pt−O bond, estimated to be 136−225 kJ/mol and ∼350 kJ/mol, respectively,[26] at equilibrium coverage, one would conclude that sulfate and bisulfate anions that provide two or three bonding oxygen atoms should be the dominant species at increasingly positive potentials. Indeed, in situ vibrational spectroscopy studies[16,23,31] confirmed the adsorption of sulfate ions on the Pt surface and its increase with potential, with no sulfate desorption. EC-STM studies on flat single crystals (e.g., Pt, Au, Pd, and Cu)[19,21,46] also provide evidence for sulfate adsorption, or more accurately coadsorption of water and (bi)sulfate ions, forming superstructures on the electrode surfaces. Our XAS measurements on Au electrodes (Figure S6) confirm the occurrence of sulfate adsorption and the concomitant accumulation of H_3O^+ at the Au−H_2SO_4(aq) interface.

The differences between the conclusions from our XAS results and those from other electrochemical studies may arise from the fact that our XAS measurements are performed while holding the voltage steady during the data acquisition at each voltage for about 20 min. As a result, our results more closely report the thermodynamic equilibrium structure at that voltage. This is fundamentally different from the transient, rate-dependent CV measurements, which probe the slow dynamics of physical or chemical transformations.

4. CONCLUSIONS

Using interface-sensitive *operando* EY-XAS, together with MD simulations, continuum modeling, and XAS simulations, we could determine the chemical structure and speciation in the electric double layer at the Pt−H_2SO_4(aq) interface in the potential range above the hydrogen evolution and below the oxygen evolution reactions. We have demonstrated that for positive electrode potentials the surface is decorated with sulfate (SO_4^{2-}) ions with nearby H_3O^+ in the first few layers (depending on the voltage) with no appreciable contribution of bisulfate or sulfuric acid (HSO_4^-, H_2SO_4). We have also shown that Pt−O/Pt−OH does not form at least up to 1.3 V. In addition to a more complete determination of the EDL structure and composition, our study demonstrates the power of surface sensitive and element specific EY-XAS experiments combined with first-principles theory to probe the structure of buried, solid−liquid, functional electrochemical interfaces with molecular-scale detail. It solidifies the connections between time- and ensemble-averaged XAS measurements and the underlying thermodynamic mechanism for adsorption of species from the electrolyte to the electrode surface. These results open the way for future atomistic studies of the chemistry of interfaces relevant to electrochemistry and its applications to electrolysis, fuel cells, and energy storage, from batteries to supercapacitors.

■ ASSOCIATED CONTENT

Supporting Information

The Supporting Information is available free of charge on the ACS Publications website at DOI: 10.1021/jacs.8b09743.

More details regarding materials and thin film preparation, experimental configuration of *operando* XAS measurements, XAS spectra analysis, saturation effects, FPMD and XAS spectra simulations, modeling of biased interfaces using continuum models, and supporting figures (S1−S15) (PDF)

■ AUTHOR INFORMATION

Corresponding Author

*mbsalmeron@lbl.gov

ORCID

Cheng Hao Wu: 0000-0002-6515-0988
Tod A. Pascal: 0000-0003-2096-1143
Jinghua Guo: 0000-0002-8576-2172
Miquel B. Salmeron: 0000-0002-2887-8128

Author Contributions

⊗C.H.W. and T.A.P. contributed equally to this work.

Notes

The authors declare no competing financial interest.

■ ACKNOWLEDGMENTS

This work was supported by the Office of Basic Energy Sciences (BES), Division of Materials Sciences and Engineering, of the U.S. Department of Energy (DOE) under Contract No. DE-AC02-05CH11231, through the Structure and Dynamics of Materials Interfaces program (FWP KC31SM). The X-ray absorption spectroscopy measurements were performed at the Advanced Light Source, supported by DOE under the same contract. Theory and simulations were performed within a user project at the Molecular Foundry, Lawrence Berkeley National Laboratory, supported by the DOE under the same contract number. All computations are performed using the computing resources of the National Energy Research Scientific Computing Center (NERSC), supported by the Office of Science of the U.S. Department of Energy under the same contract. We also thank Dr. C. Das Pemmaraju, Dr. Liwen F. Wan, Dr. Craig P. Schwartz, Prof. Richard J. Saykally, Dr. Philip N. Ross, Prof. Xiaofeng Feng, and Dr. Stephen J. Harris for useful discussions.

■ REFERENCES

(1) Bard, A. J.; Abruna, H. D.; Chidsey, C. E.; Faulkner, L. R.; Feldberg, S. W.; Itaya, K.; Majda, M.; Melroy, O.; Murray, R. W. The Electrode/Electrolyte Interface-A Status Report. *J. Phys. Chem.* **1993**, *97* (28), 7147−7173.

(2) Bard, A. J.; Faulkner, L. R. *Electrochemical Methods: Fundamentals and Applications*; Wiley, 1980.

DOI: 10.1021/jacs.8b09743
J. Am. Chem. Soc. XXXX, XXX, XXX−XXX

(3) Wu, C. H.; Weatherup, R. S.; Salmeron, M. B. Probing Electrode/Electrolyte Interfaces in Situ by X-Ray Spectroscopies: Old Methods, New Tricks. *Phys. Chem. Chem. Phys.* **2015**, *17* (45), 30229−30239.
(4) Angerstein-Kozlowska, H.; Conway, B. E.; Sharp, W. B. A. The Real Condition of Electrochemically Oxidized Platinum Surfaces: Part I. Resolution of Component Processes. *J. Electroanal. Chem. Interfacial Electrochem.* **1973**, *43* (1), 9−36.
(5) Conway, B. E.; Gottesfeld, S. Real Condition of Oxidized Platinum Electrodes: Part II. Resolution of Reversible and Irreversible Processes by Optical and Impedance Studies. *J. Chem. Soc., Faraday Trans. 1* **1973**, *69*, 1090.
(6) Tilak, B. V.; Conway, B. E.; Angerstein-Kozlowska, H. The Real Condition of Oxidized Pt Electrodes: Part III. Kinetic Theory of Formation and Reduction of Surface Oxides. *J. Electroanal. Chem. Interfacial Electrochem.* **1973**, *48* (1), 1−23.
(7) Kolics, A.; Wieckowski, A. Adsorption of Bisulfate and Sulfate Anions on a Pt(111) Electrode. *J. Phys. Chem. B* **2001**, *105* (13), 2588−2595.
(8) Gamboa-Aldeco, M. E.; Herrero, E.; Zelenay, P. S.; Wieckowski, A. Adsorption of Bisulfate Anion on a Pt(100) Electrode: A Comparison with Pt(111) and Pt(Poly). *J. Electroanal. Chem.* **1993**, *348* (1−2), 451−457.
(9) Wieckowski, A.; Kolics, A. Comments on 'On the Calculation of Surface Concentration from the Measurement by the Radiotracer "Electrode Lowering" Technique' by D. Poskus. *J. Electroanal. Chem.* **1999**, *464* (1), 118−122.
(10) Jerkiewicz, G.; Vatankhah, G.; Lessard, J.; Soriaga, M. P.; Park, Y. S. Surface-Oxide Growth at Platinum Electrodes in Aqueous H2SO4 Reexamination of Its Mechanism through Combined Cyclic-Voltammetry, Electrochemical Quartz-Crystal Nanobalance, and Auger Electron Spectroscopy Measurements. *Electrochim. Acta* **2004**, *49* (9−10), 1451−1459.
(11) Kongkanand, A.; Ziegelbauer, J. M. Surface Platinum Electrooxidation in the Presence of Oxygen. *J. Phys. Chem. C* **2012**, *116* (5), 3684−3693.
(12) Kim, J.; Urchaga, P.; Baranton, S.; Coutanceau, C.; Jerkiewicz, G. Interfacial Structure of Atomically Flat Polycrystalline Pt Electrodes and Modified Sauerbrey Equation. *Phys. Chem. Chem. Phys.* **2017**, *19* (33), 21955−21963.
(13) Kolb, D. M. Electrochemical Surface Science. *Angew. Chem., Int. Ed.* **2001**, *40*, 1162−1181.
(14) Shen, Y. R.; Ostroverkhov, V. Sum-Frequency Vibrational Spectroscopy on Water Interfaces: Polar Orientation of Water Molecules at Interfaces. *Chem. Rev.* **2006**, *106* (4), 1140−1154.
(15) Osawa, M.; Tsushima, M.; Mogami, H.; Samjeské, G.; Yamakata, A. Structure of Water at the Electrified Platinum−Water Interface: A Study by Surface-Enhanced Infrared Absorption Spectroscopy. *J. Phys. Chem. C* **2008**, *112* (11), 4248−4256.
(16) Braunschweig, B.; Mukherjee, P.; Dlott, D. D.; Wieckowski, A. Real-Time Investigations of Pt(111) Surface Transformations in Sulfuric Acid Solutions. *J. Am. Chem. Soc.* **2010**, *132* (40), 14036−14038.
(17) Toney, M. F.; Howard, J. N.; Richer, J.; Borges, G. L.; Gordon, J. G.; Melroy, O. R.; Wiesler, D. G.; Yee, D.; Sorensen, L. B. Voltage-Dependent Ordering of Water Molecules at an Electrode-Electrolyte Interface. *Nature* **1994**, *368* (6470), 444.
(18) Nagy, Z.; You, H. Applications of Surface X-Ray Scattering to Electrochemistry Problems. *Electrochim. Acta* **2002**, *47* (19), 3037−3055.
(19) Climent, V.; Feliu, J. M. Thirty Years of Platinum Single Crystal Electrochemistry. *J. Solid State Electrochem.* **2011**, *15* (7−8), 1297−1315.
(20) Markovic, N.; Schmidt, T. J.; Marković, N. M.; Schmidt, T. J.; Stamenković, V.; Ross, P. N. Oxygen Reduction Reaction on Pt and Pt Bimetallic Surfaces: A Selective Review. *Fuel Cells* **2001**, *1* (2), 105−116.
(21) Braunschweig, B.; Daum, W. Superstructures and Order-Disorder Transition of Sulfate Adlayers on Pt(111) in Sulfuric Acid Solution. *Langmuir* **2009**, *25* (18), 11112−11120.
(22) Jerkiewicz, G. Hydrogen Sorption at/in Electrodes. *Prog. Surf. Sci.* **1998**, *57* (2), 137−186.
(23) Kunimatsu, K.; Samant, M. G.; Seki, H. In-Situ FT-IR Spectroscopic Study of Bisulfate and Sulfate Adsorption on Platinum Electrodes Part 1. Sulfuric Acid. *J. Electroanal. Chem. Interfacial Electrochem.* **1989**, *258* (1), 163−177.
(24) Savich, W.; Sun, S.-G.; Lipkowski, J.; Wieckowski, A. Determination of the Sum of Gibbs Excesses of Sulfate and Bisulfate Adsorbed at the Pt(111) Electrode Surface Using Chronocoulometry and Thermodynamics of the Perfectly Polarized Electrode. *J. Electroanal. Chem.* **1995**, *388* (1−2), 233−237.
(25) Kunimatsu, K.; Samant, M. G.; Seki, H.; Philpott, M. R. A Study of HSO_4^- and SO_4^{2-} Co-Adsorption on a Platinum Electrode in Sulfuric Acid by in-Situ Ft-Ir Reflection Absorption Spectroscopy. *J. Electroanal. Chem. Interfacial Electrochem.* **1988**, *243* (1), 203−208.
(26) Markovic, N. M.; Ross, P. N., Jr. Surface Science Studies of Model Fuel Cell Electrocatalysts. *Surf. Sci. Rep.* **2002**, *45* (4−6), 117−229.
(27) Redmond, E. L.; Setzler, B. P.; Alamgir, F. M.; Fuller, T. F. Elucidating the Oxide Growth Mechanism on Platinum at the Cathode in PEM Fuel Cells. *Phys. Chem. Chem. Phys.* **2014**, *16* (11), 5301−5311.
(28) Teliska, M.; O'Grady, W. E.; Ramaker, D. E. Determination of O and OH Adsorption Sites and Coverage in Situ on Pt Electrodes from Pt L_{23} X-Ray Absorption Spectroscopy. *J. Phys. Chem. B* **2005**, *109* (16), 8076−8084.
(29) Faguy, P. W.; Marinković, N. S.; Adžić, R. R. Infrared Spectroscopic Analysis of Anions Adsorbed from Bisulfate-Containing Solutions on Pt(111) Electrodes. *J. Electroanal. Chem.* **1996**, *407* (1−2), 209−218.
(30) Sawatari, Y.; Inukai, J.; Ito, M. The Structure of Bisulfate and Perchlorate on a Pt(111) Electrode Surface Studied by Infrared Spectroscopy and Ab-Initio Molecular Orbital Calculation. *J. Electron Spectrosc. Relat. Phenom.* **1993**, *64*−*65* (C), 515−522.
(31) Kunimatsu, K.; Samant, M. G.; Seki, H. In-Situ FT-IR Spectroscopic Study of Bisulfate and Sulfate Adsorption on a Platinum Electrode. Part 2. Mildly Acid and Alkaline Sodium Sulfate Solutions. *J. Electroanal. Chem. Interfacial Electrochem.* **1989**, *272* (1−2), 185−194.
(32) Lachenwitzer, A.; Li, N.; Lipkowski, J. Determination of the Acid Dissociation Constant for Bisulfate Adsorbed at the Pt(111) Electrode by Subtractively Normalized Interfacial Fourier Transform Infrared Spectroscopy. *J. Electroanal. Chem.* **2002**, *532* (1−2), 85−98.
(33) Velasco-Velez, J. J.; Wu, C. H.; Pascal, T. A.; Wan, L. F.; Guo, J.; Prendergast, D.; Salmeron, M. The Structure of Interfacial Water on Gold Electrodes Studied by X-Ray Absorption Spectroscopy. *Science* **2014**, *346*, 831−834.
(34) Zheng, H.; Meng, Y. S.; Zhu, Y. Frontiers of in Situ Electron Microscopy. *MRS Bull.* **2015**, *40* (01), 12−18.
(35) Nemšák, S.; Shavorskiy, A.; Karslioglu, O.; Zegkinoglou, I.; Rattanachata, A.; Conlon, C. S.; Keqi, A.; Greene, P. K.; Burks, E. C.; Salmassi, F.; et al. Concentration and Chemical-State Profiles at Heterogeneous Interfaces with Sub-Nm Accuracy from Standing-Wave Ambient-Pressure Photoemission. *Nat. Commun.* **2014**, *5*, 5441.
(36) Axnanda, S.; Crumlin, E. J.; Mao, B.; Rani, S.; Chang, R.; Karlsson, P. G.; Edwards, M. O. M.; Lundqvist, M.; Moberg, R.; Ross, P.; et al. Using "Tender" X-Ray Ambient Pressure X-Ray Photoelectron Spectroscopy as A Direct Probe of Solid-Liquid Interface. *Sci. Rep.* **2015**, *5*, 9788.
(37) Kumar, S.; Bouzida, D.; Swendsen, R. H.; Kollman, P. A.; Rosenberg, J. M. The Weighted Histogram Analysis Method for Free-Energy Calculations on Biomolecules. I. The Method. *J. Comput. Chem.* **1992**, *13* (8), 1011−1021.
(38) Torrie, G. M.; Valleau, J. P. Nonphysical Sampling Distributions in Monte Carlo Free-Energy Estimation: Umbrella Sampling. *J. Comput. Phys.* **1977**, *23*, 187−199.
(39) Baskin, A.; Prendergast, D. Improving Continuum Models to Define Practical Limits for Molecular Models of Electrified Interfaces. *J. Electrochem. Soc.* **2017**, *164* (11), E3438−E3447.
(40) Prendergast, D.; Galli, G. X-Ray Absorption Spectra of Water from First Principles Calculations. *Phys. Rev. Lett.* **2006**, *96* (21), 215502.

DOI: 10.1021/jacs.8b09743
J. Am. Chem. Soc. XXXX, XXX, XXX−XXX

(41) England, A. H.; Duffin, A. M.; Schwartz, C. P.; Uejio, J. S.; Prendergast, D.; Saykally, R. J. On the Hydration and Hydrolysis of Carbon Dioxide. *Chem. Phys. Lett.* **2011**, *514* (4−6), 187−195.
(42) Ramaswamy, N.; Mukerjee, S. Fundamental Mechanistic Understanding of Electrocatalysis of Oxygen Reduction on Pt and Non-Pt Surfaces: Acid versus Alkaline Media. *Adv. Phys. Chem.* **2012**, *2012*, 1−17.
(43) Nilsson, A.; Nordlund, D.; Waluyo, I.; Huang, N.; Ogasawara, H.; Kaya, S.; Bergmann, U.; Näslund, L.-Å.; Öström, H.; Wernet, P.; et al. X-Ray Absorption Spectroscopy and X-Ray Raman Scattering of Water and Ice; an Experimental View. *J. Electron Spectrosc. Relat. Phenom.* **2010**, *177* (2−3), 99−129.
(44) Comas-Vives, A.; Bandlow, J.; Jacob, T. Ab Initio Study of the Electrochemical H_2SO_4/Pt(111) Interface. *Phys. Chem. Chem. Phys.* **2013**, *15* (3), 992−997.
(45) Santana, J.; Cabrera, C.; Ishikawa, Y. A density-functional theory study of electrochemical adsorption of sulfuric acid anions on Pt(111). *Phys. Chem. Chem. Phys.* **2010**, *12*, 9526−9534.
(46) Kim, Y. G.; Soriaga, J. B.; Vigh, G.; Soriaga, M. P. Atom-Resolved EC-STM Studies of Anion Adsorption at Well-Defined Surfaces: Pd(111) in Sulfuric Acid Solution. *J. Colloid Interface Sci.* **2000**, *227* (2), 505−509.
(47) Luzar, A.; Chandler, D. Hydrogen-Bond Kinetics in Liquid Water. *Nature* **1996**, *379*, 55.
(48) Miller, D. J.; Öberg, H.; Kaya, S.; Sanchez Casalongue, H.; Friebel, D.; Anniyev, T.; Ogasawara, H.; Bluhm, H.; Pettersson, L. G. M.; Nilsson, A. Oxidation of Pt(111) under Near-Ambient Conditions. *Phys. Rev. Lett.* **2011**, *107* (19), 195502.

DOI: 10.1021/jacs.8b09743
J. Am. Chem. Soc. XXXX, XXX, XXX−XXX